THE JOURNAL OF BIOLOGICAL CHEMISTRY VOL. 289, NO. 18, pp. 12195–12201, May 2, 2014

Structure-guided Mutation of the Conserved G3-box Glycine in Rheb Generates a Constitutively Activated Regulator of Mammalian Target of Rapamycin (mTOR)*

Received for publication, December 19, 2013, and in revised form, March 11, 2014
Published, JBC Papers in Press, March 19, 2014, DOI 10.1074/jbc.C113.543736

Mohammad T. Mazhab-Jafari, Christopher B. Marshall, Jason Ho, Noboru Ishiyama, Vuk Stambolic, and Mitsuhiko Ikura[1]

From the Campbell Family Cancer Research Institute, Princess Margaret Cancer Centre and, Department of Medical Biophysics, University of Toronto, Toronto, Ontario M5G 2M9, Canada

Background: GTPases regulate cellular signaling by cycling between GDP-(inactive) and GTP-(active) bound states.
Results: Rheb GTPase cycling was manipulated by structure-guided mutagenesis of an ultraconserved residue.
Conclusion: Constitutively activated or inactive Rheb mutants were generated by substitutions that displace the hydrolytic water or γ-phosphate, respectively.
Significance: These mutants offer new research tools, and the approach may be extended to other GTPases.

Constitutively activated variants of small GTPases, which provide valuable functional probes of their role in cellular signaling pathways, can often be generated by mutating the canonical catalytic residue (*e.g.* Ras Q61L) to impair GTP hydrolysis. However, this general approach is ineffective for a substantial fraction of the small GTPase family in which this residue is not conserved (*e.g.* Rap) or not catalytic (*e.g.* Rheb). Using a novel engineering approach, we have manipulated nucleotide binding through structure-guided substitutions of an ultraconserved glycine residue in the G3-box motif (D*XX*G). Substitution of Rheb Gly-63 with alanine impaired both intrinsic and TSC2 GTPase-activating protein (GAP)-mediated GTP hydrolysis by displacing the hydrolytic water molecule, whereas introduction of a bulkier valine side chain selectively blocked GTP binding by steric occlusion of the γ-phosphate. Rheb G63A stimulated phosphorylation of the mTORC1 substrate p70S6 kinase more strongly than wild-type, thus offering a new tool for mammalian target of rapamycin (mTOR) signaling.

The Ras superfamily comprises 167 members, which share a common fold, and function as "switches" to regulate diverse cellular signaling pathways (1). Small GTPases cycle between an activated GTP-bound state that interacts with and activates downstream effector proteins to drive signaling and an inactive GDP-bound state. Thus, GTPases are inactivated by hydrolysis of the γ-phosphate of GTP and can be reactivated by exchange of GDP for a new molecule of GTP, processes that occur slowly, but are catalyzed by the upstream regulators GTPase-activating proteins (GAPs)[2] and guanine nucleotide exchange factors (GEFs), respectively. Mutations that impair GTP hydrolysis perturb this cycle and generate hyperactivated variants (*e.g.* Ras G12V and Q61L) that are often associated with disease processes. Nevertheless, constitutively activated and inactive GTPase mutants are indispensable research tools for probing the function of GTPases and dissecting the signaling pathways they regulate. The strategy most widely used to generate activated GTPases employs point mutations of a solvent-exposed glutamine residue in the G3-box motif (2) in switch II (five G-boxes comprise conserved sequence elements for nucleotide binding and effector recognition). This glutamine is conserved in 73% of human GTPases (3) and has been demonstrated to be a key catalytic residue in several cases. Structural and enzymatic studies of Ras have shown that the carboxamide oxygen of this glutamine side chain (Gln-61) catalyzes GTP hydrolysis by increasing the nucleophilicity of a hydrolytic water molecule (H_2O^{cat}) positioned in-line with the γ-phosphate (4). Although this mechanism is conserved among many GTPases, this residue is substituted in one-quarter of small GTPases, and in some Ras superfamily members, this glutamine is present but noncatalytic. These GTPases have lower catalytic activity, which may proceed through alternate mechanisms. In Ras homolog enriched in brain (Rheb), the G3-box glutamine residue (Gln-64) is found in a noncatalytic conformation, and its mutation has no impact on intrinsic hydrolysis and only modestly reduces GAP-mediated hydrolysis (5–7). Mutations of Ras Gly-12 impair GTP hydrolysis because the presence of a side chain restricts the proper alignment of the catalytic residue; however, Rheb already has a bulky residue (Arg-15) in this position, and its mutation has little effect on hydrolysis (6). Thus, despite the modest impact of the Q64L mutation, it remains well used for lack of a more robust activated Rheb variant (7–10). In mutagenic analyses of residues potentially mediating the noncanonical catalytic mechanism of Rheb, mutation of Asp-65 had the greatest impact on catalytic activity (11); however, the reduction in intrinsic GTPase activity was limited to a modest ~30% (D65A). Tuberous sclerosis complex 2 (TSC2) possesses a GAP activity that accelerates the intrinsic GTP hydrolysis of wild-type Rheb (6, 12). Mutation of Rheb Asp-65

* This work was supported by the Cancer Research Society (Canada), Canadian Cancer Society Research Institute Grant 2010-700494, and the Princess Margaret Cancer Foundation.
The atomic coordinates and structure factors (codes 4O25, 4O2L, and 4O2R) have been deposited in the Protein Data Bank (http://wwpdb.org/).
[1] Holds the Canada Research Chair. To whom correspondence should be addressed. E-mail: mikura@uhnres.utoronto.ca.

[2] The abbreviations used are: GAP, GTPase-activating protein; Rheb, Ras homolog enriched in brain; TSC, tuberous sclerosis complex; mTOR, mammalian target of rapamycin; mTORC1, mammalian target of rapamycin complex 1; H_2O^{cat}, catalytic water; GEF, guanine nucleotide exchange factor; S6K, S6 kinase; MEF, mouse embryonic fibroblast; r.m.s.d., root mean square deviation; HSQC, heteronuclear single-quantum coherence.

also impaired sensitivity to TSC2 GAP, but Rheb D65A did not fully activate mammalian target of rapamycin complex 1 (mTORC1), possibly due to weakened interaction (11). Therefore, we sought to develop novel strategies to control the GTPase cycle of Rheb and other GTPase proteins that lack the canonical catalytic machinery.

EXPERIMENTAL PROCEDURES

Protein Preparation—Mus musculus Rheb (residues 1–169) WT and G63A and G63V mutants and TSC2 GAP domain (residues 1,525–1,742) were expressed as glutathione *S*-transferase (GST) fusions from the pGEX2T vector in *Escherichia coli* (BL21 strain) as described previously (13). Briefly, bacteria were grown in minimal M9 media supplemented with either $^{14}NH_4Cl$ or $^{15}NH_4Cl$ at 37 °C to $A_{600} = 0.6$, and protein expression was initiated with 0.25 mM isopropyl-1-thio-β-D-galactopyranoside at 15 °C. Mutations were introduced using QuikChange site-directed mutagenesis (Stratagene). The proteins were affinity-purified using glutathione-Sepharose, cleaved from the GST tag by thrombin, and further purified using Superdex 75 (GE Healthcare) size exclusion chromatography. Human Rap1A (residues 1–167) was expressed using pET28 vector and purified using nickel-nitrilotriacetic acid resin followed by removal of the His tag with thrombin and further purification by Superdex 75 size exclusion chromatography. Small GTPase proteins expressed in *E. coli* were co-purified with guanine nucleotide.

NMR-based Real-time GTPase Assay—For GTP hydrolysis assays, the small GTPase proteins were loaded with GTP in the presence of EDTA and 10-fold excess GTP, and following the addition of $MgCl_2$, excess reagents were removed by passage through a desalting column (PD MidiTrap G-25; GE Healthcare) equilibrated with NMR buffer (20 mM Tris, pH 7.4, 100 mM NaCl, 5 mM $MgCl_2$, and 1 mM Tris(2-carboxyethyl) phosphine hydrochloride). The final protein concentration used in NMR experiments was 0.3 mM. The proteins were fully GTP-loaded at the start of each assay, as judged by ^{1}H-^{15}N heteronuclear single-quantum coherence (HSQC) spectrum. Prior to nucleotide exchange assays, the GTPase proteins were incubated at room temperature for a minimum of a week and monitored by ^{1}H-^{15}N HSQC spectra to ensure that *E. coli*-derived GTP had hydrolyzed, and then exchange reactions were initiated by the addition of 1.5 mM GTP (5-fold molar excess). For GAP assays, TSC2 GAP domain was added to the GTP-loaded Rheb (WT or mutant) at a molar ratio of 1:2.

All NMR spectra were acquired on Bruker AVANCE II 800-MHz spectrometer equipped with a 5-mm TCI CryoProbe or a 600-MHz spectrometer with a TCI 1.7-mm MicroCryoProbe. ^{1}H-^{15}N HSQC spectra with sensitivity enhancement were collected in succession with four scans (10-min acquisition time) to monitor the GTPase reaction at 293.2 K. Spectral processing was carried out with NMRPipe (14), and the nucleotide-sensitive peaks were integrated via Gaussian line fitting using SPARKY (15). Residues exhibiting distinct and well resolved peaks for each nucleotide-bound state were monitored as reporters of the reaction rates, as described previously (6). For each pair of reporter resonances, the fraction of protein in the GDP-bound state was calculated as $I_{GDP}/(I_{GDP} + I_{GTP})$, where I represents intensity, plotted against time and fit to one-phase exponential decay or association functions for nucleotide exchange and hydrolysis, respectively. The error was estimated as described previously (6). Because resonance assignments are not available for Rap1A GTPase, the fraction of protein in the GDP-bound state was calculated as $I_{GDP}{}^{avg}/(I_{GDP}{}^{avg} + I_{GTP}{}^{avg})$, where $I_{GDP}{}^{avg}$ and $I_{GTP}{}^{avg}$ represent the average intensities of GDP- and GTP-specific peaks. The error was then estimated from spectral noise and propagated accordingly. Data fitting was performed with Prism (GraphPad software).

Crystallization and Data Collection—Crystals of Rheb (residues 1–169) WT, G63A, and G63V mutants were grown with seeding using the hanging drop vapor diffusion method at room temperature. The protein solution contained 0.8 mM protein, 20 mM Tris-HCl (pH 8.0), 200 mM NaCl, 5 mM $MgCl_2$, and 0.02% NaN3 w/v. The protein solution was mixed with an equal volume of the well solution (100 mM Tris-HCl (pH 8.5), 200 mM sodium acetate trihydrate, and 30% w/v polyethylene glycol 4000). Crystals of Rheb WT and G63A mutant were soaked in a solution containing 20 mM GTP and 25% polyethylene glycol 400 for 2 h at room temperature to allow nucleotide exchange, whereas G63V crystals were soaked in 25% polyethylene glycol 400 alone. Crystals were then flash-frozen in liquid nitrogen. Diffraction data (WT and G63A) were collected at 100 K on a Rigaku FR-E super-bright rotating anode generator equipped with a Rigaku Saturn A200 CCD detector, Osmic VariMax HF optics, and an Oxford cryosystem with a wavelength of 1.54 Å at the Structural Genomics Consortium, Toronto, and processed with HKL2000 (16). Rheb WT GTP and G63A GTP diffracted to a resolution of 2.2 and 2.40 Å, respectively. The diffraction data for Rheb G63V GDP was collected at 100 K with copper Kα radiation on a Bruker Microstar X8 PROTEUM SMART CCD system with a wavelength of 1.54 Å to a resolution of 2.25 Å and processed with the PROTEUM suite of programs.

Structure Determination and Refinement—The structures of GTP-bound murine Rheb WT and G63A were solved by molecular replacement using the structure of human Rheb WT in GTP-bound conformation (PDB: 1XTS) as the initial search model, whereas the structure of murine Rheb G63V in complex with GDP was solved using the structure of human Rheb in GDP-bound conformation (PDB: 1XTQ). The final models were generated after successive rounds of refinements using PHENIX (17) accompanied by manual model building with Coot (18). During the course of refinement, densities for the nucleotides and the hydrolytic water molecules (in the case of Rheb WT) were clearly visible in difference electron density maps, which enabled us to manually position the molecules. WT and mutant proteins were crystallized with two Rheb molecules in the asymmetric unit, with one of the switch I and II regions of the molecule being involved in the crystal packing. All the structures discussed in this study are from the Rheb molecules where the switches I and II are not involved in crystal packing, except for the GDP-bound Rheb G63V, where the electron density of switch II was weak in the absence of crystal contact but well resolved upon crystal contact formation. It is worthwhile to note that switch II in GDP-bound Rheb G63V adopted a similar conformation to the GDP-bound Rheb WT (PDB: 1XTQ). The Ramachandran statistics of the final

TABLE 1
Data collection and refinement statistics
Statistical information regarding the crystal structures of Rheb WT and G63A mutant in GTP-bound form and G63V mutant in GDP-bound form.

	Rheb-WT-GTP	Rheb-G63A-GTP	Rheb-G63V-GDP
Data collection			
Space group	P 2 2_1 2_1	P 2 2_1 2_1	P 2_1 2_1 2
Cell dimensions			
a, *b*, *c* (Å)	57.7, 70.5, 79.8	57.6, 70.2, 79.7	70.3, 79.2, 57.3
α, β, γ (°)	90, 90, 90	90, 90, 90	90, 90, 90
Resolution (Å)	50.0-2.20 (2.24-2.20)[a]	50.0-2.40 (2.44-2.40)[a]	50-2.25 (2.35-2.25)[a]
R_{sym}	0.127 (0.549)	0.155 (0.574)	0.073 (0.344)
$I/\sigma I$	15 (4.1)	14.9 (3.8)	12.3 (3.4)
Completeness (%)	99.0 (98.6)	100 (100)	99.9 (100)
Redundancy	7.0 (7.1)	7.7 (7.8)	13 (8.0)
Refinement			
Resolution (Å)	39.9-2.2	38.9-2.4	28.7-2.25
No. of reflections	15,674	12,371	14,672
R_{work}/R_{free}	20.3/25.6	19.5/24.3	20.6/25.9
No. atoms			
Protein	2738	2736	2742
Ligand/Mg^{2+} ion	62/2	62/2	54/2
Water	130	119	125
B-factors			
Protein	25.2	30.7	21.9
Ligand/ion	26.4	33.3	17.8
Water	28.1	34.3	23.1
r.m.s.d.			
Bond lengths (Å)	1.04	1.11	1.13
Bond angles (°)	0.007	0.008	0.008
Ramachandran statistics			
Most Favorable region (%)	94.8	95.1	94.6
Allowed region (%)	5.2	4.9	5.4
Disallowed region (%)	0	0	0

[a] Data set was collected from one crystal. Values in parentheses are for highest resolution shell.

models were as follows: 94.2, 95.1, and 93.9% of the residues were in the preferred region for Rheb WT GTP, Rheb G63A GTP, and Rheb G63V GDP. The remainder of the residues, for each model, were in the allowed region with no outliers. The data collection and refinement statistics can be found in Table 1.

Cell-based Phosphorylation Assays—Antibodies against p70 S6 Kinase and its Thr-389-phosphorylated form were from Cell Signaling Technology, and the M2-FLAG antibody was from Sigma. Murine Rheb cDNA (Open Biosystems) was subcloned into FLAG-tagged pcDNA5. The mutant Rheb construct was generated via site-directed mutagenesis (Agilent). Myc-p70 S6K was cloned in to pcDNA3.1. The p70 S6K phosphorylation assays were performed according to a previously described protocol (11) with the following modifications. In brief, 3×10^5 HeLa H1 and 2.7×10^6 $TSC2^{-/-}$ MEF cells, cultured in Dulbecco's modified Eagle's medium containing 10% fetal calf serum (DMEM/10% FCS), were co-transfected with FLAG-Rheb WT or G63A and Myc-S6K at a ratio of 20:1 using Effectene (Qiagen) and 5:1 using GenJet reagent (SignaGen) for HeLa H1 and MEF cells, respectively. Twenty-four hours after transfection, the media were exchanged with serum-free DMEM. Forty-eight hours after transfection, cells were either further starved or stimulated with 100 nM insulin for 15 min prior to harvesting. FLAG-Rheb and Myc-S6K were immunoprecipitated from normalized lysates with anti-FLAG and anti-Myc antibodies and protein A/G mix PureProteome magnetic beads (Millipore) for Western blot analysis.

RESULTS AND DISCUSSION

The hydrolytic H_2O^{cat} has been observed in almost all high-resolution GTPase structures. It is coordinated by hydrogen bonds with the γ-phosphate of GTP and a common set of highly conserved residues including the backbone carbonyl of a threonine in the G2-box and the backbone amide of a glycine in the G3-box. The threonine (Thr-35 in Ras) is in the C-terminal part of switch I and is 90% identical among human GTPases (3), whereas the glycine (Gly-60 in Ras, 93% identity) (3) is in the N-terminal part switch II. The curved-loop configuration of the G3-box D*XX*G motif (where *X* stands for any amino acid) allows the aspartic acid to coordinate a Mg^{2+} ion required for nucleotide binding (19) and positions the Cα of the glycine next to H_2O^{cat} and proximal to the γ-phosphate (1). On the basis of this structure, we hypothesized that by substituting various residues for glycine, we could introduce side-chain steric clashes to selectively perturb binding of the H_2O^{cat} and/or the γ-phosphate. Displacing the H_2O^{cat} would impair GTP hydrolysis, yielding an activated variant, whereas blocking γ-phosphate binding would yield an inactive mutant that can only accommodate GDP. We first applied this novel engineering approach to the mTOR activator Rheb (Fig. 1*A*), examining how mutations of Gly-63 affect its noncanonical GTPase cycle.

Real-time NMR-based GTPase assays (6) demonstrated that mutation of Gly-63 to alanine substantially reduced the intrinsic GTP hydrolysis rate of Rheb by ~4.5-fold, (Fig. 1*B*), consistent with our notion that the introduction of a methyl side chain could destabilize the H_2O^{cat}. Most remarkably, no TSC2 GAP activity could be detected for the Rheb G63A mutant (Fig. 1*B*), which was predicted because GAP-catalyzed hydrolysis utilizes the same H_2O^{cat}, stimulating the reaction by stabilizing and complementing the intrinsic catalytic machinery. Finally, to investigate whether the mutation affects intrinsic nucleotide exchange of GDP for GTP, we carried out real-time NMR

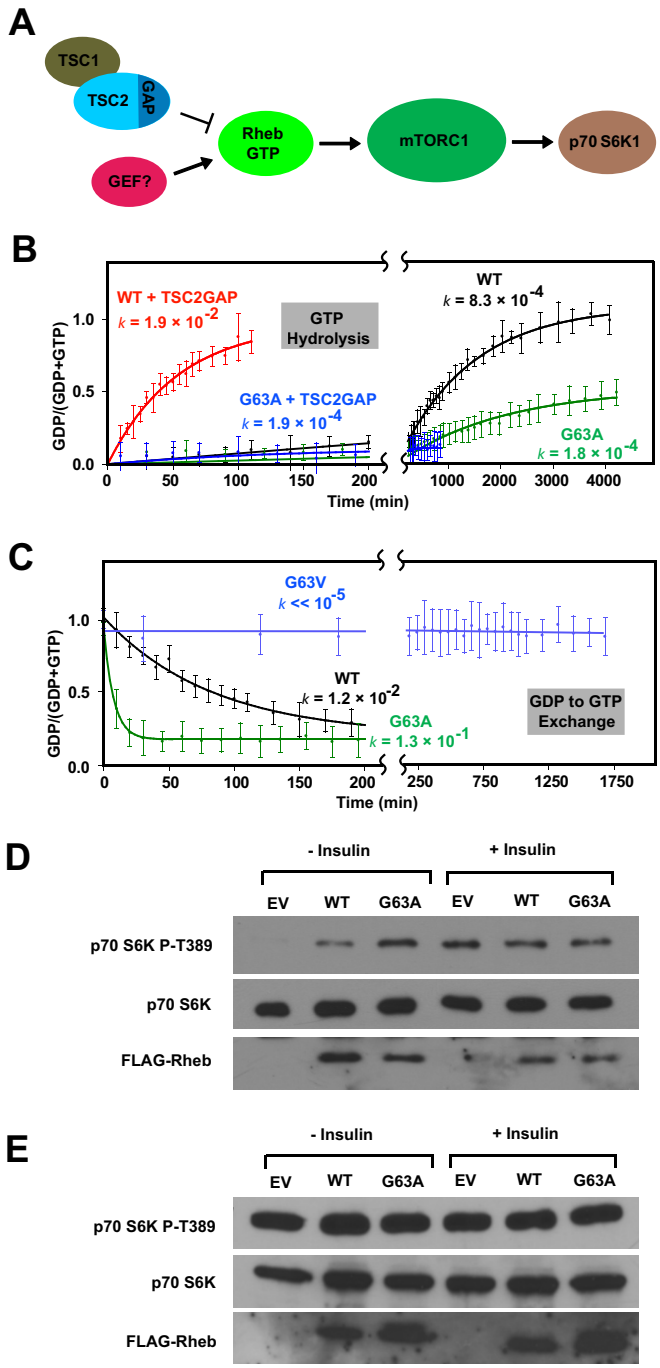

FIGURE 1. **Manipulation of the GTPase cycle of Rheb and mTOR signaling through substitutions of Gly-63.** *A*, schematic illustration of the mTORC1 signaling pathway. Rheb GTP stimulates the kinase activity of mTORC1, which phosphorylates substrates including 4EBP1 and p70S6K1 that promote protein biosynthesis and cell cycle progression. The GAP activity of TSC2 catalyzes hydrolysis of GTP to inactivate Rheb, and TSC2 is regulated by the availability of growth factors and energy. The identity and existence of a GEF for Rheb have not been resolved. Translationally controlled tumor protein (TCTP) (27), protein associated with Myc (PAM) (28), and soluble $\alpha\beta$-tubulin (29) have been proposed as Rheb GEFs; however, such a role for TCTP has been disputed (30, 31). *B*, hydrolysis of GTP by wild-type Rheb and G63A in the presence and absence of the TSC2 GAP domain, monitored by real-time NMR. *Error bars* represent standard deviation of the fraction of GDP ($I_{GDP}/(I_{GDP} + I_{GTP})$) reported by 10 residues. *C*, intrinsic nucleotide exchange (GDP to GTP) of wild-type Rheb, G63A, and G63V. Reaction rates are in min^{-1}. *D* and *E*, Rheb G63A mutation increases activation of mTORC1 signaling under starvation. HeLa cells (*D*) and TSC2-deficient MEF cells (*E*) were transfected with wild-type Rheb, G63A, or empty vector (*EV*) and starved or stimulated with insulin prior to lysis. Each experiment was performed in duplicate with one representative blot shown.

exchange assays. Rheb G63A exchanged >10 times faster than the wild-type protein (Fig, 1C), and although this effect was not anticipated *a priori*, it would further drive this mutant toward the activated state. Conversely, mutation of Gly-63 to valine resulted in a Rheb variant that failed to bind GTP (Fig. 1*C*), consistent with steric interference between the bulkier side chain and the γ-phosphate. As expected, Rheb G63V remained fully GDP-bound and inactive. Therefore, we have identified a single, highly conserved residue whose mutation can result in two diametrically opposed effects on activation.

Rheb activates mTORC1, which regulates protein biosynthesis, cell growth, proliferation, and autophagy (20–22). Consistent with our biochemical data (Fig. 1*B*), overexpression of Rheb G63A in HeLa cells stimulated phosphorylation of the mTORC1 kinase substrate p70 S6K more strongly than wild-type Rheb in the absence of serum, when TSC2 is active (Fig. 1*D*). Upon serum stimulation, which inactivates TSC2, p70 S6K is highly phosphorylated, and its phosphorylation cannot be further enhanced by expression of wild-type or G63A Rheb, suggesting that under this condition, p70 S6K phosphorylation is limited by mTORC1 rather than the availability of endogenous Rheb GTP (Fig. 1*D*). Similarly, the high level of p70 S6K phosphorylation in TSC2-null MEFs cannot be further enhanced by expression of wild-type or G63A Rheb (Fig. 1*E*). Although Rheb G63V expressed well in *E. coli*, in mammalian cells its expression was ~90% lower than the wild type (data not shown); thus, we could not reliably probe the effects of this mutation on mTORC1 signaling. Reduced expression of nucleotide-free Rheb mutants has been reported previously (7). The inability to bind GTP, which is much more abundant than GDP in mammalian cells (23), might explain the poor expression of G63V, despite the stability of its GDP-bound form.

To validate that these mutations of the ultraconserved G3-box glycine (Fig. 2*A*) exert their effects through the anticipated mechanisms, we solved the crystal structures of wild-type Rheb and the G63A mutant bound to GTP and of the Rheb G63V mutant bound to GDP (Figs. 2, *B–D*, and 3, *A–C*). The overall fold was not substantially affected by the mutations (all atoms r.m.s.d. WT GTP *versus* G63A GTP = 0.23 Å and WT GDP (5) *versus* G63V GDP = 0.74 Å); however, the electron density of the nucleotide-binding pocket confirmed the positioning of the Ala-63 side chain in the H_2O^{cat}-γ-phosphate-binding cavity of the mutant (Figs. 2*C* and 3*B*). Although the electron density of the H_2O^{cat} is clearly visible in the WT structure, no corresponding density is observed in the G63A mutant structure (Fig. 3, *A* and *B*). Hence we hypothesize that the reduced residency of the hydrolytic H_2O^{cat} decreases the ability of the G63A mutant to hydrolyze GTP, in full agreement with the biochemical observations. In the structure of Rheb G63V in complex with GDP, the bulkier valine side chain occupies additional space within the nucleotide-binding pocket. Val-63 Cγ was positioned less than 2 Å from the γ-phosphate location determined in the GTP-bound wild-type structure (Figs. 2*D* and 3*C*). Thus, enthalpic costs and steric clashes prevent the γ-phosphate from approaching the methyl protons, explaining the lack of GTP binding and nucleotide exchange for Rheb G63V.

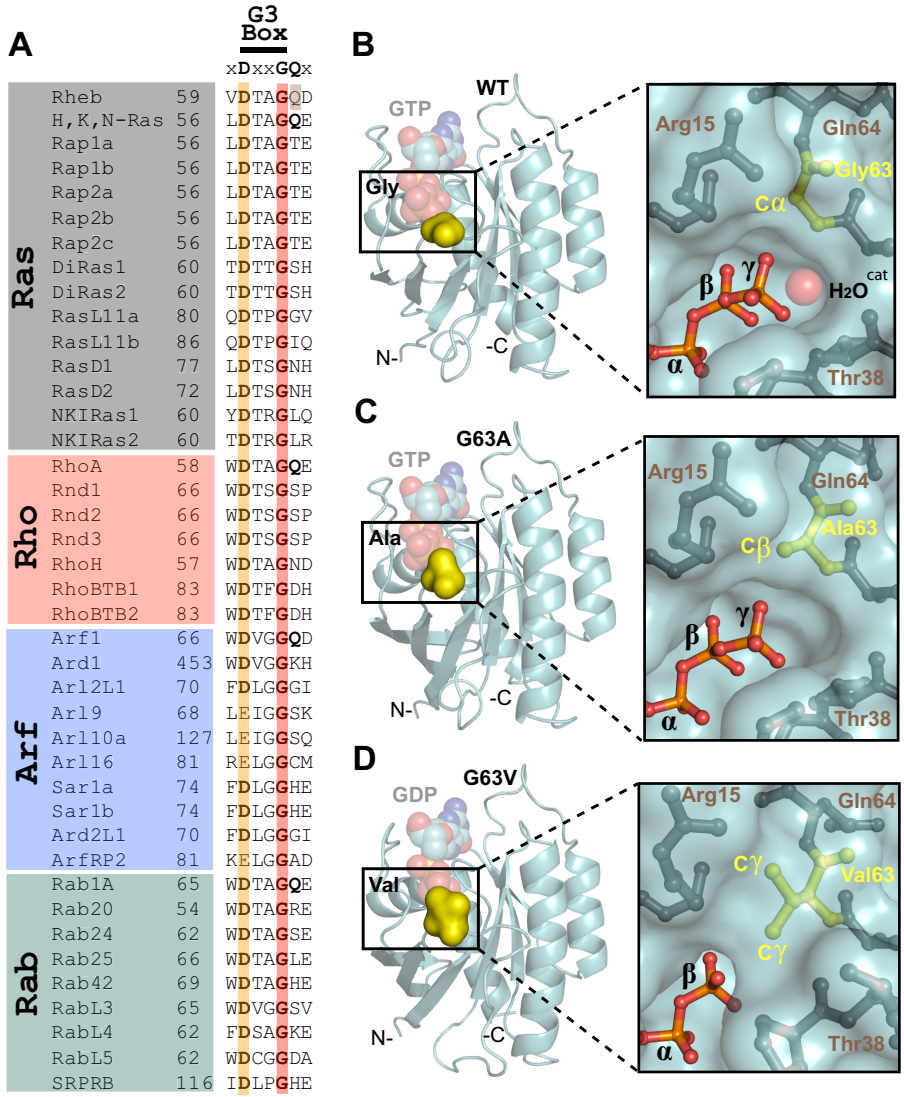

FIGURE 2. **Conservation of the G3-box glycine and structural basis for the functional properties of Rheb G63A/G63V mutants.** *A*, alignment of the G3-boxes of selected small GTPase protein sequences illustrating conservation of the Gly residue. GTPases lacking the catalytic glutamine residue were selected. *B–D*, overall fold of wild-type Rheb GTP (*B*), Rheb G63A GTP (*C*), and Rheb G63V GDP (*D*), with each nucleotide-binding site enlarged (*right*). The nucleotide is represented with *spheres* (*left*) or *balls-and-sticks* (*right*), and the glycine, alanine, and valine are shown in *yellow*. For clarity, Tyr-35 is not shown.

Previously, an analogous substitution (G60A) in Ras was biochemically and structurally characterized. This G60A mutation reduced the intrinsic GTP hydrolysis rate of Ras as well; however, this was mediated by a distinct mechanism involving substantial distortions of both switch regions that displace the catalytic glutamine away from the nucleotide-binding site by ~5–8 Å (24). This conformation resembled that of nucleotide-free Ras in complex with its exchange factor Son of Sevenless (SOS) (24–26), and consequently, Ras G60A was shown to exert a dominant negative effect in cells by forming a stable nonproductive complex with SOS that sequesters this GEF (24, 26). In contrast, the switch I and II regions of Rheb retain the wild-type conformation in the G63A mutant structure (all atoms r.m.s.d. of 0.22 and 0.35 Å for switch I and II, respectively). Thus, the *in vivo* phenotypes of G3-box glycine mutants are GTPase-specific and must be characterized. Nevertheless, the ability to generate gain-of-function mutants for some non-canonical GTPases is especially valuable for developing probes. We therefore investigated the effect of substituting Gly-60 in Rap1A (37% sequence identity with Rheb), a small GTPase for which no mutation impairing GTP hydrolysis is available because the canonical catalytic glutamine is replaced by a threonine. The G60A mutation reduced the GTP hydrolysis rate of Rap1A by 3-fold (Fig. 4*A*), which is remarkable considering that no other mutation has been reported to inactivate Rap GTPase activity. In the case of Rap1A, however, the G60V mutation did not perturb nucleotide exchange activity (Fig. 4*B*), suggesting that the valine side chain adopts a different conformation from that of Rheb G63V. Hence the structural and functional properties of G3-box glycine mutations should be investigated for each GTPase. Intriguingly, a few examples of G3-box Gly residue mutations have been listed in the catalogue of somatic mutations in cancer (COSMIC) database (K-Ras G60A/G60V/G60D, H-Ras G60S, and Rheb G63W). Although these muta-

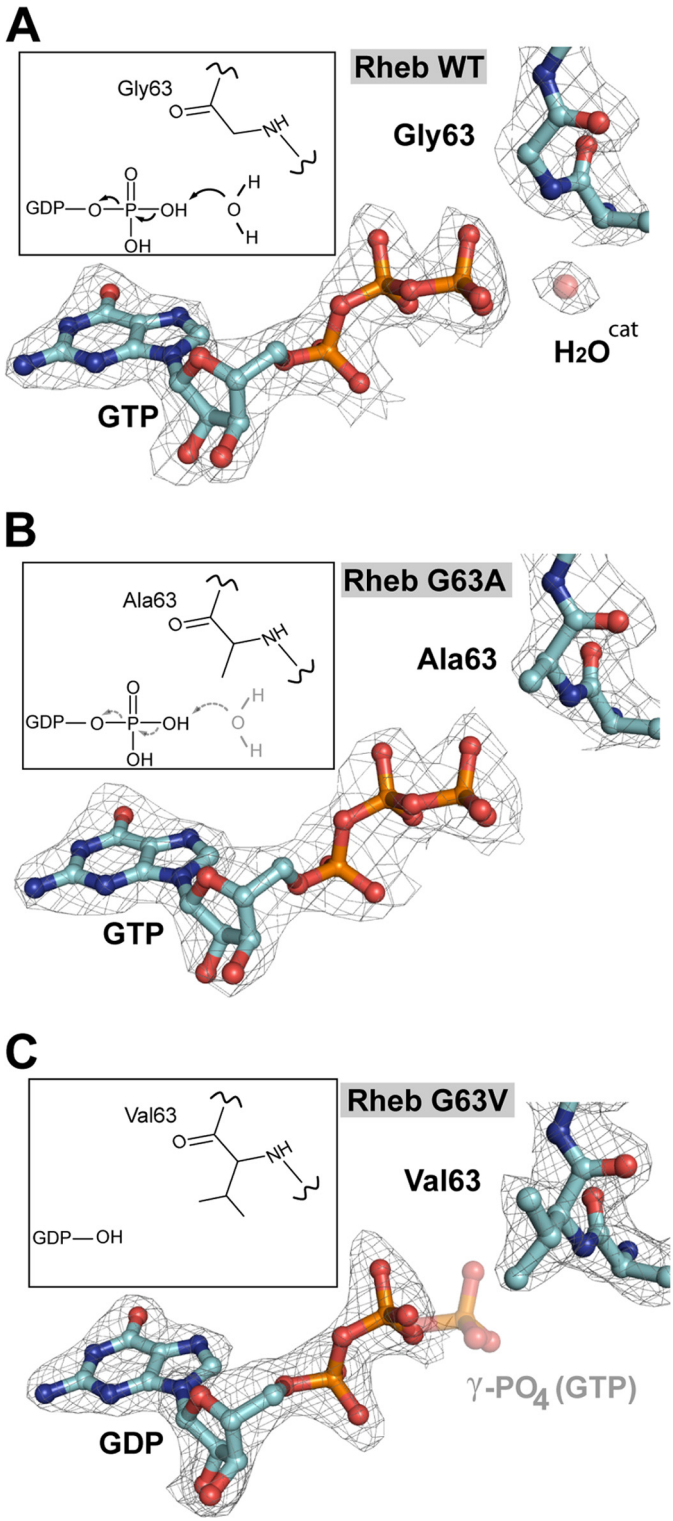

FIGURE 3. **Electron densities of the catalytic sites of wild-type Rheb and its Gly-63 mutations.** *A–C*, $2F_o - F_c$ electron density maps of the nucleotide and residue 63 at 1.0σ are shown for Rheb WT GTP (*A*), Rheb G63A GTP (*B*), and Rheb G63V GDP (*C*). The $2F_o - F_c$ electron density map of the hydrolytic water is shown at 1.0σ in *A*, but is absent in *B* and *C*. The predicted position of the γ-phosphate, based on global alignment of Rheb WT GTP with Rheb G63V GDP, is indicated in *C* (*semitransparent*). The *insets* in each panel are chemical schematics illustrating the relative positions of the γ-phosphate, the G3-box glycine (the mutated alanine and valine), the hydrolytic water, and the nucleophilic GTPase reaction.

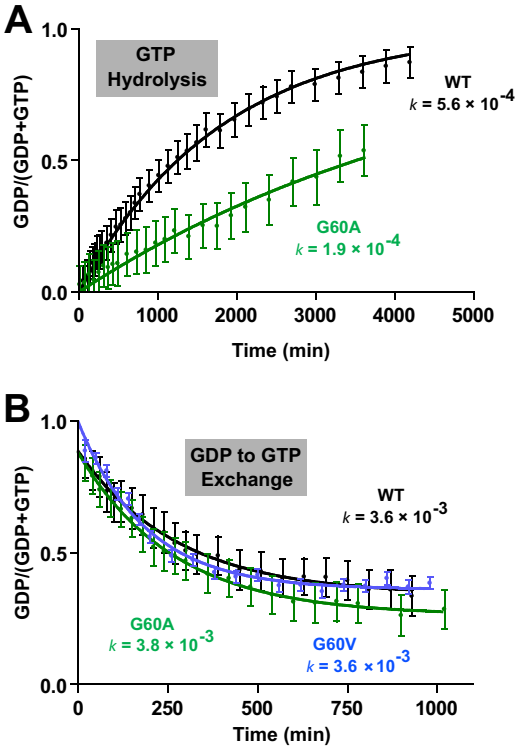

FIGURE 4. **Intrinsic nucleotide hydrolysis and exchange of Rap1A GTPase and its Gly-60 mutations.** *A*, GTP hydrolysis by wild-type Rap1A (*black*) and the G60A mutant (*green*). *B*, GDP to GTP exchange monitored for wild-type Rap1A (*black*) and the G60A (*green*) and G60V (*blue*) mutants. Reaction rates derived by curve fitting are shown with the same color codes (in min^{-1}). *Error bars* represent standard deviation of the fraction of GDP ($I_{GDP}/(I_{GDP} + I_{GTP})$) reported by 10 residues.

tions were identified in colon, thyroid, and hematopoietic cancers, it remains to be determined whether they are oncogenic "driver" mutations.

In this study, we have successfully demonstrated a structure-guided approach whereby mutating a single residue in the conserved G3-box can control nucleotide binding, thereby locking Rheb in an activated (G63A GTP) or an inactive (G63V GDP) conformation. In serum-starved HeLa cells, the G63A mutant strongly activated the downstream effector mTORC1, thus enhancing p70 S6K phosphorylation, whereas the inability to bind GTP rendered G63V unstable in these cells. The crystal structures of the two Rheb mutants provided the structural basis for the unique features of each mutant. To our knowledge this is the first report of a mutation that severely impairs GTP hydrolysis of GTPases with noncanonical catalytic mechanisms. This diverse group of GTPases includes several members from four of the five GTPase subfamilies: Ras, Rab, Rho, and Arf (Fig. 2*A*); thus, this strategy should be a valuable biological tool for probing the functions of these unique proteins.

Acknowledgments—We thank Aiping Dong from the Structural Genomics Consortium and Doug Kuntz for x-ray data collection. NMR spectrometers were funded by the Canada Foundation for Innovation.

REFERENCES

1. Wittinghofer, A., and Vetter, I. R. (2011) Structure-function relationships of the G domain, a canonical switch motif. *Annu. Rev. Biochem.* **80,**

943–971
2. Der, C. J., Finkel, T., and Cooper, G. M. (1986) Biological and biochemical properties of human *ras*^{H} genes mutated at codon 61. *Cell* **44,** 167–176
3. Wennerberg, K., Rossman, K. L., and Der, C. J. (2005) The Ras superfamily at a glance. *J. Cell Sci.* **118,** 843–846
4. Frech, M., Darden, T. A., Pedersen, L. G., Foley, C. K., Charifson, P. S., Anderson, M. W., and Wittinghofer, A. (1994) Role of glutamine-61 in the hydrolysis of GTP by p21H-ras: an experimental and theoretical study. *Biochemistry* **33,** 3237–3244
5. Yu, Y., Li, S., Xu, X., Li, Y., Guan, K., Arnold, E., and Ding, J. (2005) Structural basis for the unique biological function of small GTPase RHEB. *J. Biol. Chem.* **280,** 17093–17100
6. Marshall, C. B., Ho, J., Buerger, C., Plevin, M. J., Li, G. Y., Li, Z., Ikura, M., and Stambolic, V. (2009) Characterization of the intrinsic and TSC2-GAP-regulated GTPase activity of Rheb by real-time NMR. *Sci. Signal.* **2,** ra3
7. Li, Y., Inoki, K., and Guan, K. L. (2004) Biochemical and functional characterizations of small GTPase Rheb and TSC2 GAP activity. *Mol. Cell. Biol.* **24,** 7965–7975
8. Jiang, H., and Vogt, P. K. (2008) Constitutively active Rheb induces oncogenic transformation. *Oncogene* **27,** 5729–5740
9. Zhou, X., Ikenoue, T., Chen, X., Li, L., Inoki, K., and Guan, K. L. (2009) Rheb controls misfolded protein metabolism by inhibiting aggresome formation and autophagy. *Proc. Natl. Acad. Sci. U.S.A.* **106,** 8923–8928
10. Mavrakis, K. J., Zhu, H., Silva, R. L., Mills, J. R., Teruya-Feldstein, J., Lowe, S. W., Tam, W., Pelletier, J., and Wendel, H. G. (2008) Tumorigenic activity and therapeutic inhibition of Rheb GTPase. *Genes Dev.* **22,** 2178–2188
11. Mazhab-Jafari, M. T., Marshall, C. B., Ishiyama, N., Ho, J., Di Palma, V., Stambolic, V., and Ikura, M. (2012) An autoinhibited noncanonical mechanism of GTP hydrolysis by Rheb maintains mTORC1 homeostasis. *Structure* **20,** 1528–1539
12. Inoki, K., Li, Y., Xu, T., and Guan, K. L. (2003) Rheb GTPase is a direct target of TSC2 GAP activity and regulates mTOR signaling. *Genes Dev.* **17,** 1829–1834
13. Marshall, C. B., Meiri, D., Smith, M. J., Mazhab-Jafari, M. T., Gasmi-Seabrook, G. M., Rottapel, R., Stambolic, V., and Ikura, M. (2012) Probing the GTPase cycle with real-time NMR: GAP and GEF activities in cell extracts. *Methods* **57,** 473–485
14. Delaglio, F., Grzesiek, S., Vuister, G. W., Zhu, G., Pfeifer, J., and Bax, A. (1995) NMRPipe: a multidimensional spectral processing system based on UNIX pipes. *J. Biomol. NMR* **6,** 277–293
15. Goddard, T. D., and Kneller, D. (2008) *SPARKY 3*, University of California, San Francisco
16. Otwinowski, Z., and Minor, W. (1997) Processing of x-ray diffraction data collected in oscillation mode. *Methods Enzymol.* **276,** 307–326
17. Adams, P. D., Afonine, P. V., Bunkóczi, G., Chen, V. B., Davis, I. W., Echols, N., Headd, J. J., Hung, L. W., Kapral, G. J., Grosse-Kunstleve, R. W., McCoy, A. J., Moriarty, N. W., Oeffner, R., Read, R. J., Richardson, D. C., Richardson, J. S., Terwilliger, T. C., and Zwart, P. H. (2010) PHENIX: a comprehensive Python-based system for macromolecular structure solution. *Acta Crystallogr. D Biol. Crystallogr.* **66,** 213–221
18. Emsley, P., and Cowtan, K. (2004) Coot: model-building tools for molecular graphics. *Acta Crystallogr. D Biol. Crystallogr.* **60,** 2126–2132
19. John, J., Rensland, H., Schlichting, I., Vetter, I., Borasio, G. D., Goody, R. S., and Wittinghofer, A. (1993) Kinetic and structural analysis of the Mg^{2+}-binding site of the guanine nucleotide-binding protein $p21^{H\text{-}ras}$. *J. Biol. Chem.* **268,** 923–929
20. Stocker, H., Radimerski, T., Schindelholz, B., Wittwer, F., Belawat, P., Daram, P., Breuer, S., Thomas, G., and Hafen, E. (2003) Rheb is an essential regulator of S6K in controlling cell growth in *Drosophila*. *Nat. Cell Biol.* **5,** 559–565
21. Saucedo, L. J., Gao, X., Chiarelli, D. A., Li, L., Pan, D., and Edgar, B. A. (2003) Rheb promotes cell growth as a component of the insulin/TOR signalling network. *Nat. Cell Biol.* **5,** 566–571
22. Kim, J., Kundu, M., Viollet, B., and Guan, K. L. (2011) AMPK and mTOR regulate autophagy through direct phosphorylation of Ulk1. *Nat. Cell Biol.* **13,** 132–141
23. Traut, T. W. (1994) Physiological concentrations of purines and pyrimidines. *Mol. Cell Biochem.* **140,** 1–22
24. Ford, B., Skowronek, K., Boykevisch, S., Bar-Sagi, D., and Nassar, N. (2005) Structure of the G60A mutant of Ras: implications for the dominant negative effect. *J. Biol. Chem.* **280,** 25697–25705
25. Boriack-Sjodin, P. A., Margarit, S. M., Bar-Sagi, D., and Kuriyan, J. (1998) The structural basis of the activation of Ras by Sos. *Nature* **394,** 337–343
26. Sung, Y. J., Hwang, M. C., and Hwang, Y. W. (1996) The dominant negative effects of H-Ras harboring a Gly to Ala mutation at position 60. *J. Biol. Chem.* **271,** 30537–30543
27. Hsu, Y. C., Chern, J. J., Cai, Y., Liu, M., and Choi, K. W. (2007) i TCTP is essential for growth and proliferation through regulation of dRheb GTPase. *Nature* **445,** 785–788
28. Maeurer, C., Holland, S., Pierre, S., Potstada, W., and Scholich, K. (2009) Sphingosine-1-phosphate induced mTOR-activation is mediated by the E3-ubiquitin ligase PAM. *Cell. Signal.* **21,** 293–300
29. Lee, M. N., Koh, A., Park, D., Jang, J. H., Kwak, D., Jeon, H., Kim, J., Choi, E. J., Jeong, H., Suh, P. G., and Ryu, S. H. (2013) Deacetylated $\alpha\beta$-tubulin acts as a positive regulator of Rheb GTPase through increasing its GTP-loading. *Cell. Signal.* **25,** 539–551
30. Wang, X., Fonseca, B. D., Tang, H., Liu, R., Elia, A., Clemens, M. J., Bommer, U. A., and Proud, C. G. (2008) Re-evaluating the roles of proposed modulators of mammalian target of rapamycin complex 1 (mTORC1) signaling. *J. Biol. Chem.* **283,** 30482–30492
31. Rehmann, H., Brüning, M., Berghaus, C., Schwarten, M., Köhler, K., Stocker, H., Stoll, R., Zwartkruis, F. J., and Wittinghofer, A. (2008) Biochemical characterisation of TCTP questions its function as a guanine nucleotide exchange factor for Rheb. *FEBS Lett.* **582,** 3005–3010